A twin amplifier for drift chambers readout

E. Botta[a], D. Calvo[b], P. Cerello[b], C. Fanara[c]
S. Marcello[b], O. Morra[d]

May 22, 1996

[a] *Dip. di Fisica Sperimentale*, Università di Torino, and INFN, Sez. di Torino, Torino, Italy.
[b] INFN, Sez. di Torino, Torino, Italy.
[c] Politecnico di Torino, and INFN, Sez. di Torino, Torino, Italy.
[d] CNR, Istituto di Cosmogeofisica, and INFN, Sez. di Torino, Torino, Italy.

Abstract

A twin amplifier for drift chambers having a doublet of anode wires with the aim of solving the left-right ambiguity has been developed. Chambers of this type, working with a $He - iC_4H_{10}$ mixture, will be used by the FINUDA spectrometer at $DA\Phi NE$. This dedicated amplifier, which subtracts the induced positive signal from the direct negative one, reduces the noise on the electronic chain and cancels the common noise from external sources. Results of laboratory and beam tests, showing that this amplifier can improve the signal to noise ratio, are presented.

1 Introduction

Drift chambers are a popular component of high energy physics experiments. Generally, thousands of wires, with associated electronics, allow to reconstruct the particle trajectories and to solve the left-right ambiguity with the staggering method by means of considerable redundancy: therefore the front-end electronics design aims at a high reliability with low cost.

The FINUDA apparatus [1, 2] is a non focusing magnetic spectrometer with cylindrical geometry whose construction was approved for continuous running at $DA\Phi NE$, the Φ Factory [3] that will be operational at $INFN-LNF$ next year. The main goal of the experiment [1] is the fine spectroscopy of Λ- hypernuclei produced after the K^- capture at rest by nuclear targets and the study of the following non-mesonic decay. The most demanding feature of the apparatus is the momentum resolution on the charged particles ($\Delta p/p \leq 0.3\%$ for $p \sim 250 \div 300\ MeV/c$), over a solid angle of $\sim 2\pi\ sr$.

To achieve this goal a composite tracking device, constituted by one octagonal layer of silicon double-sided μ-strips, two octagonal layers of Low Mass Drift Chambers (LMDCs) [4, 5] and a six layer array of Straw Tubes, has been designed.

The full apparatus is immersed into a He atmosphere, to minimize the multiple Coulomb scattering, and will operate inside a superconducting solenoid providing a field of induction $B = 1.1\ T$, homogeneous within 1% over the full tracking volume. In this device the most dangerous source contributing to worsen the momentum resolution is the multiple Coulomb scattering: to minimize it, besides operating the drift chambers with He based mixtures and using very thin ($6\,\mu m$) mylar windows [7], only one layer of drift cells is used to obtain the point coordinate in space. To that purpose, a doublet of adjacent anode wires, of $25\,\mu m$ diameter and spaced by $200\,\mu m$ to solve the left-right ambiguity, is used. The wires are made of stainless steel, with a high specific resistance ($1770\ \Omega/m$) to obtain the coordinate along the wire (z coordinate) by means of the charge division method[6]. The aim was that of reaching a precision better than 1% of the wire length.

2 Circuit description

The charge division method has intrinsic limitations due to the signal to noise ratio, which limits the accuracy. In large detectors with some hundreds of long sense wires, the amplifier noise is out-weighted by others factors: difficulty to avoid ground loops in the connections of the high and low voltage power supplies, magnet power supply, integration with other spectrometer components, environmental noise due to other experiments and/or accelerators.

The moving charges, producing the pulses on the doublet of wires, give a negative signal on the closest wire and a positive induced one on the other. In order to optimize the poor signal to noise ratio, due to the small number of primary ionization pairs which is a characteristic of the $He - iC_4H_{10}$ gas mixture ($n \sim 38.5$ for a 70/30 mixture and 6 mm of track length), a dedicated twin amplifier working on both signals of the doublet has been developed.

A block diagram of the circuit is shown in fig.1. The amplifier couples the signals from the two doublet wires, adding to each one the other with inverse polarity. Supposing that a true negative pulse, due to the ionization occurring on the side of wire 1, has an amplitude S, an induced positive signal of $0.8\ S$ will appear on wire 2. After the sum stage, output 1 and 2 will provide a negative and a positive signal of amplitude $1.8\ S$. Let us now consider the response of this system to noise. For uncorrelated noise, we may assume that, if N is its amplitude on each input channel, the output amplitude will be $\sqrt{2}N$, larger than with a normal coupling. However, the signal to noise ratio for the twin amplifier will be at least $1.8\ S/\sqrt{2}N = 1.3\ S/N$, 30% better than with the normal coupling, in case of completely uncorrelated noise. Moreover, and perhaps more important, this system will automatically cancel the common noise, giving signals of the same polarity on both wires: as a consequence, an improvement greater than 30% can be obtained, depending on the significance of the common noise contribution.

The electronic circuit is presented in fig.2. The input stage is a classical low noise, low input impedance, common base amplifier [6]:

1. $R5$ gives the current/voltage amplification.

2. $R2$ and $R13$ control the steady state current to optimize the electrical characteristic of the wire to the amplifier circuit, in order to get the best signal to noise ratio.

3. The $(R2+R5)/(R9+R13)$ ratio gives the $Q1$ transistor working point (the voltage at the $Q1$ collector is $1.5\,V$). $Q2$ and $Q3$ are emitter followers which reduce the output impedance. The transistors are high frequency low noise ($7\,GHz$ gain-bandwidth).

4. A test input allows to inject a calibration signal into the amplifier.

The operational amplifier that follows the emitter follower is high speed $CLC401$ type, using current feed back: hence the frequency response is predominantly set by the feed back resistor. The voltage amplification of the output stage is ~ 15, not too big in order to maintain good rise time, linearity and stability.

3 Performance tests

3.1 Laboratory test

The performance of this amplifier has been tested in laboratory using the setup shown in fig.3. A $100\,ns$ voltage squared pulse input, sent to the test input of channel A or B, is transformed inside the amplifier by a $22\,k\Omega$ resistor in a current pulse. The output voltage vs input current characteristic is presented in fig.4: the solid line is a linear fit to the data points, from which the gain ($36.5\,mV/\mu A$) is obtained. Fig.5 shows the amplifier non linearity, defined as the difference between the expected output voltage (from the fit) and the measured one. As seen in fig.6, the deviation points have a normal distribution and this confirms that systematic deviations from linearity are negligible, less than 0.2% of the maximum output, a value compatible with the measurement errors. All the amplifiers produced for the FINUDA experiment were checked about the gain; the distribution for an input pulse of $3\,\mu A$ is shown in fig.7: the standard deviation is $\sigma = 1.19\ mV$, corresponding to an average amplification of ($36.6\ \pm 0.4\ mV/\mu A$).

Since these amplifiers will work inside a magnetic field, the temperature effects on the circuit gain have been investigated. The results are presented in fig. 8: the gain variation is $3\,mV/300\,mV$ (1%) for a ΔT of $35°\,C$. This result is in good agreement with the expected value; moreover, no effect can be observed on the signal rise time.

Since the charge division method is used for the z coordinate measurement, it is very important to keep a constant input impedance for all the amplifier channels: therefore, a careful test of all the amplifiers which will be employed during the experiment was needed. The distribution of the input impedance for 600 amplifiers, with an input stage steady current of $0.35\,mA$, is shown in fig.9: the standard deviation is $\sigma = 1.6\,\Omega$, about 1.5% of the mean value (112 Ω).

3.2 Beam test

The beam tests were carried out at the CERN PS, on a $5\,GeV/c$ π^- beam. The amplifiers were connected to the $LMDC$ prototype.

The z dispersion, i.e. the distribution of the differences between the nominal and the measured z, obtained with the normal channel amplifier and with the twin amplifier described in this paper is shown in fig. 10a and 10b, respectively. The improvement provided by the twin amplifier is clear both from the comparison of the widths and from the quality of the lorentzian fit: the resolution is about 50% better.

The rise drift time, presented in fig.11, gives an information strictly related to the precision of the hit point reconstruction. In fact, using the mixture mentioned before, whose average drift velocity is $v_d = 34\,\mu m/\,ns$, the uncertainty on the drift time is $\sim \pm 2.5\,ns$. A spatial coordinate error smaller than $100\,\mu m$ will therefore be easily accessible to the experiment, as required.

Concerning the noise, an improvement given by the cancellation of the common noise contribution (σ_{CN}) in the twin amplifier is expected. Fig. 12 shows the distribution of the input test pulses reconstructed from the amplifier output for the normal (a) and the twin (b) amplifier: the width is therefore a measurement of the electronic noise. The noise can be written as a sum of an intrinsic and a common contribution for the normal amplifier:

$$\sigma_N^2 = \sigma_i^2 + \sigma_{CN}^2 = (48.3 \pm 1.1)\ fC^2 \tag{1}$$

while for the twin amplifier it is the sum of the instrinsic contributions from the two independent channels, since the common term cancels:

$$\sigma_T^2 = 2\sigma_i^2 = (38.2 \pm 0.9)\ fC^2 \tag{2}$$

From these two equations, the contribution from the intrinsic and the common noise can be evaluated, giving the following result:

$$\sigma_i = (4.37 \pm 0.06)\ fC \qquad\qquad \sigma_{CN} = (5.4 \pm 0.1)\ fC \tag{3}$$

The improvement from the point of view of the charge resolution, in this particular experimental condition, is:

$$\frac{\sigma_N}{\sigma_T} = 1.12 \pm 0.03 \tag{4}$$

This number will increase by a further 1.8 factor coming from the sum of signals from the anode doublet during the data taking. The overall improvement on the signal/noise ratio, in the case of a common noise level similar to that of the beam test, is finally:

$$\left(\frac{S}{N}\right)_{Twin} = (2.02 \pm 0.06)\left(\frac{S}{N}\right)_{Normal} \tag{5}$$

but it is a function of the environmental common noise level.

The total noise measured during the test in terms of equivalent electrons (without shaping the output pulses) was $\sim 43000\,e$ for the normal and $\sim 38000\,e$ for the twin amplifier.

The results of these beam tests are reported in greater detail in Ref.[7].

4 Conclusions

A dedicated twin amplifier allowing to exploit at best the instrumental properties of the FINUDA Low Mass Drift Chambers has been developed. Special care has been devoted to assure stable performances. The common noise induced by environmental sources is minimized: the significant noise reduction (about a factor (1.12 ± 0.03) in the particular test experimental situation), which will improve the signal to noise ratio by a factor (2.02 ± 0.06) during the data taking in the hypothesis of a similar common noise level, reduces the drift rise time and allows a better precision on the hit reconstruction. Consequently, an improvement of $\sim 50\%$ of the resolution on the z coordinate measurement is obtained.

Quality tests on a sample of about 300 twin amplifiers (600 channels) were very satisfactory in terms of linearity, temperature coefficients and reliability.

5 Acknowledgements

Mr. V. Lunardi, Mr. D. Quarta and Mr. A. Carnino are gratefully acknowledged for their collaboration during the laboratory tests.

References

[1] The FINUDA Collaboration,*Report*, INFN Report LNF-93/021 (1993).

[2] The FINUDA Collaboration, *Technical Report*, INFN Report LNF-95/024 (1995).

[3] L. Maiani et al *The second* DAΦNE *HandBook* **I-II**, LNF-INFN (1995)

[4] G. Charpak, F. Sauli and W. Duinker, *Nucl. Instr. Meth*, **108**(1973)413.

[5] A. Breskin et al, *Nucl. Instr. Meth*, **119**(1974)9.

[6] V.Radeka et al. *IEEE Trans. on Nucl. Science* **NS-26**, (1979)

[7] M. Agnello et al, *Nucl. Instr. Meth*, **A367**(1995)100.

List of Figures

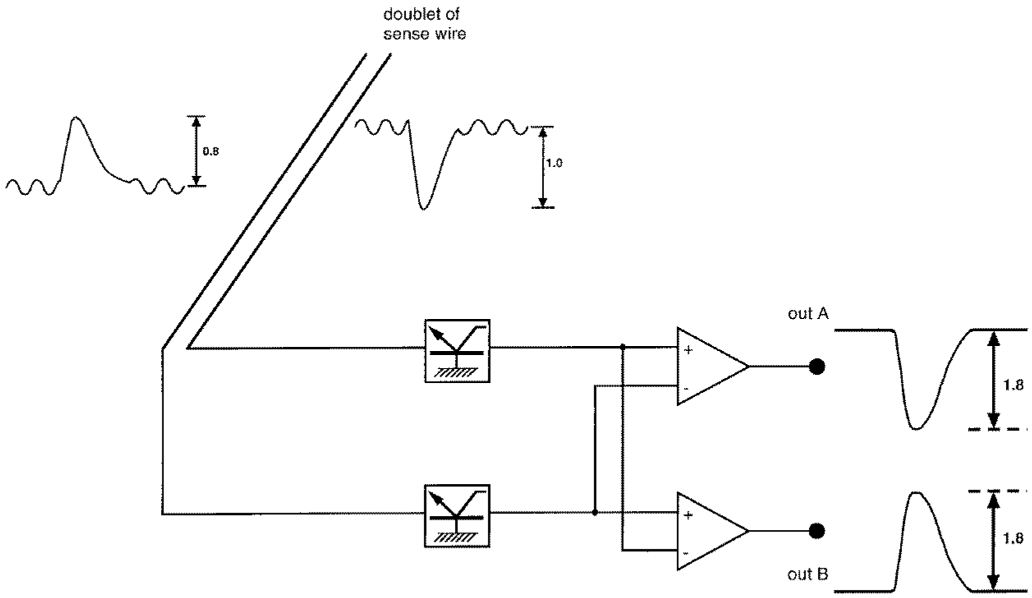

Figure 1: Block diagram of the circuit

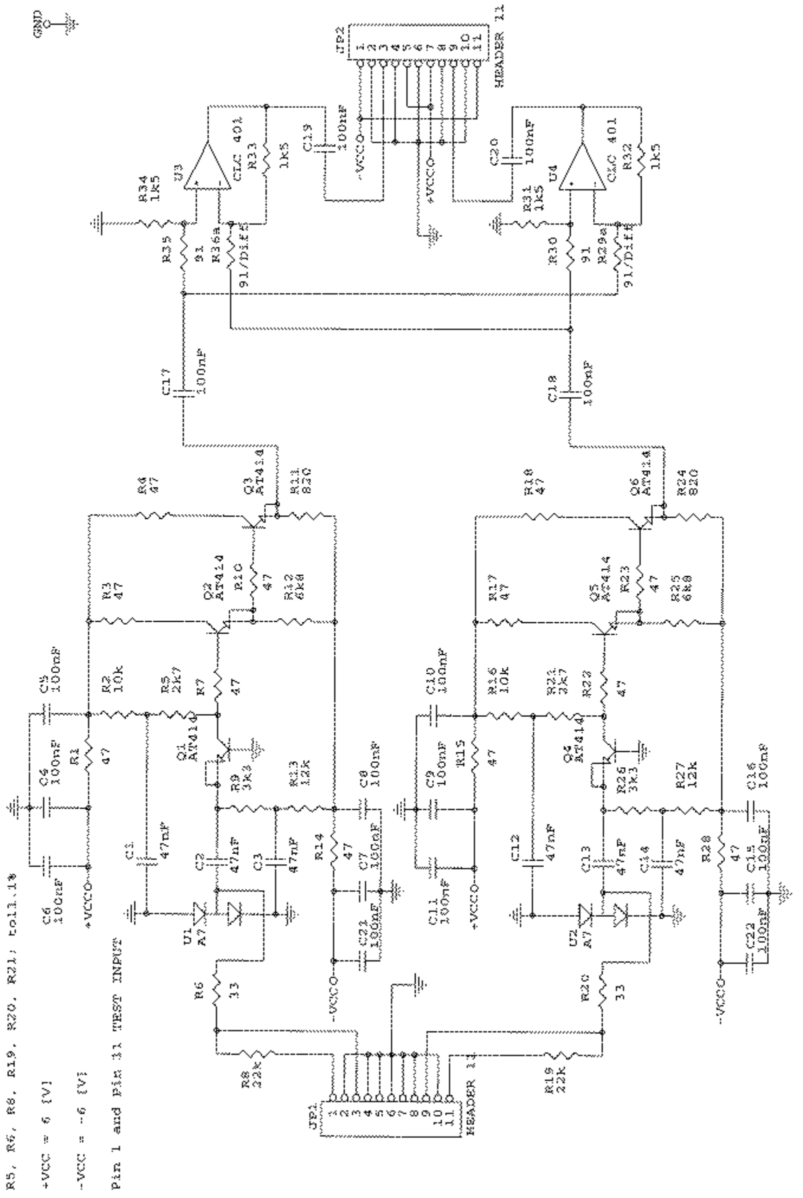

Figure 2: Electronic layout of the circuit

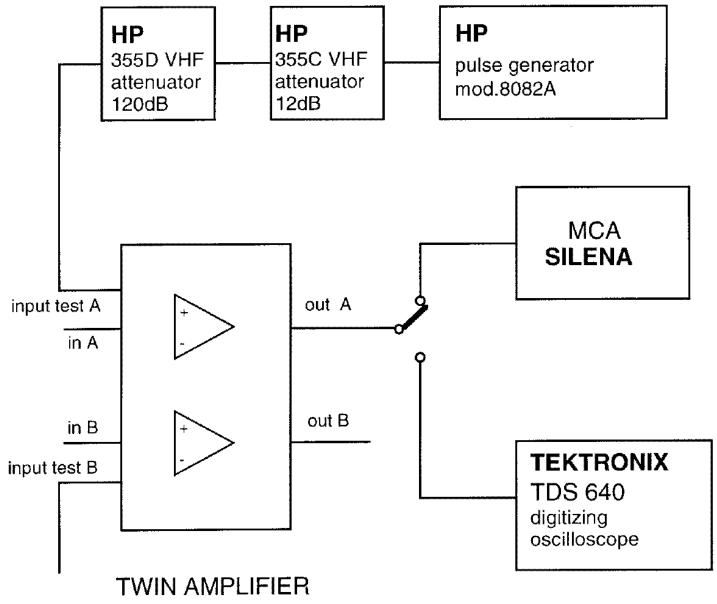

Figure 3: Laboratory test apparatus

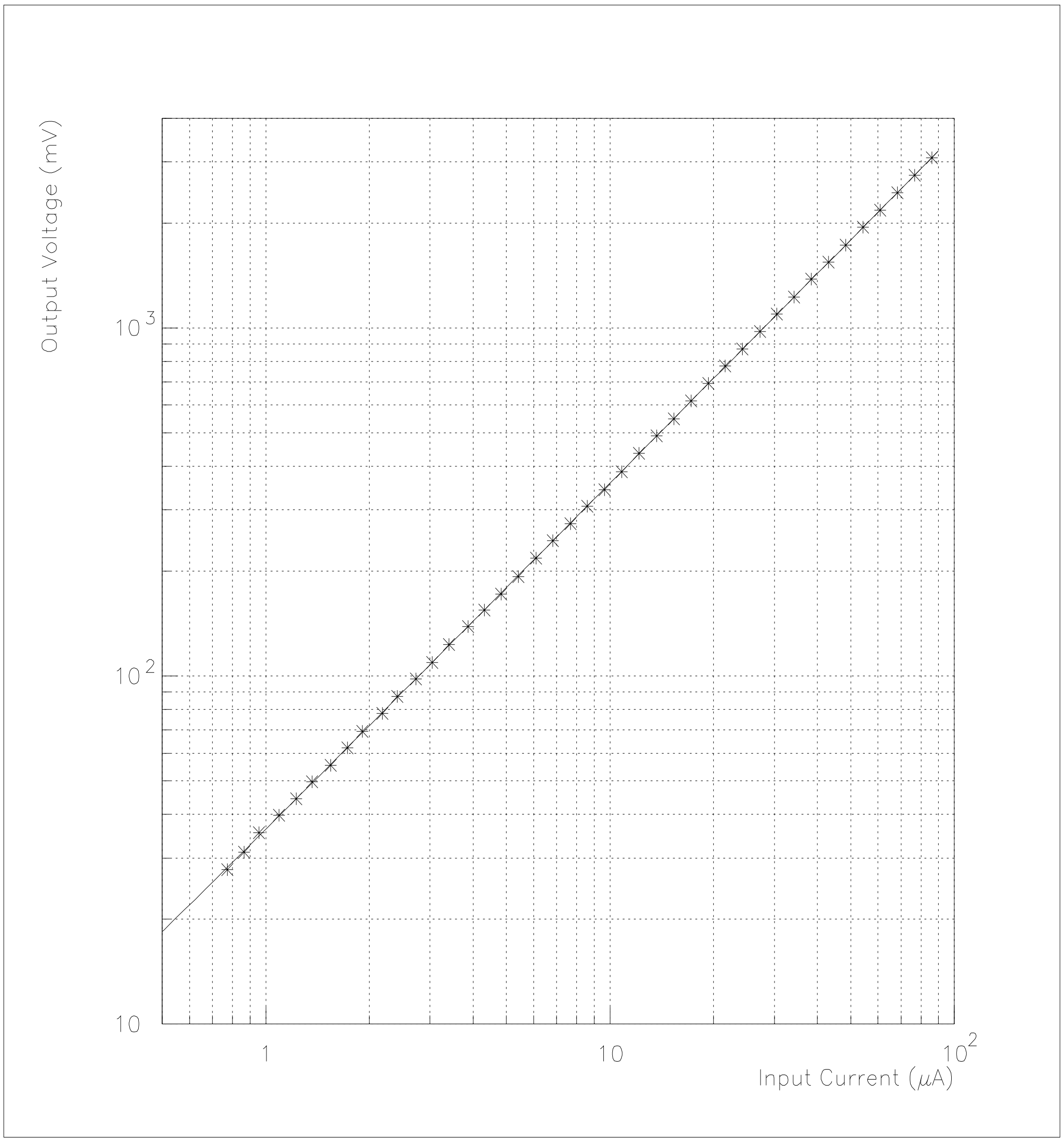

Figure 4: The gain linearity curve. Output voltage vs input current of the amplifier.

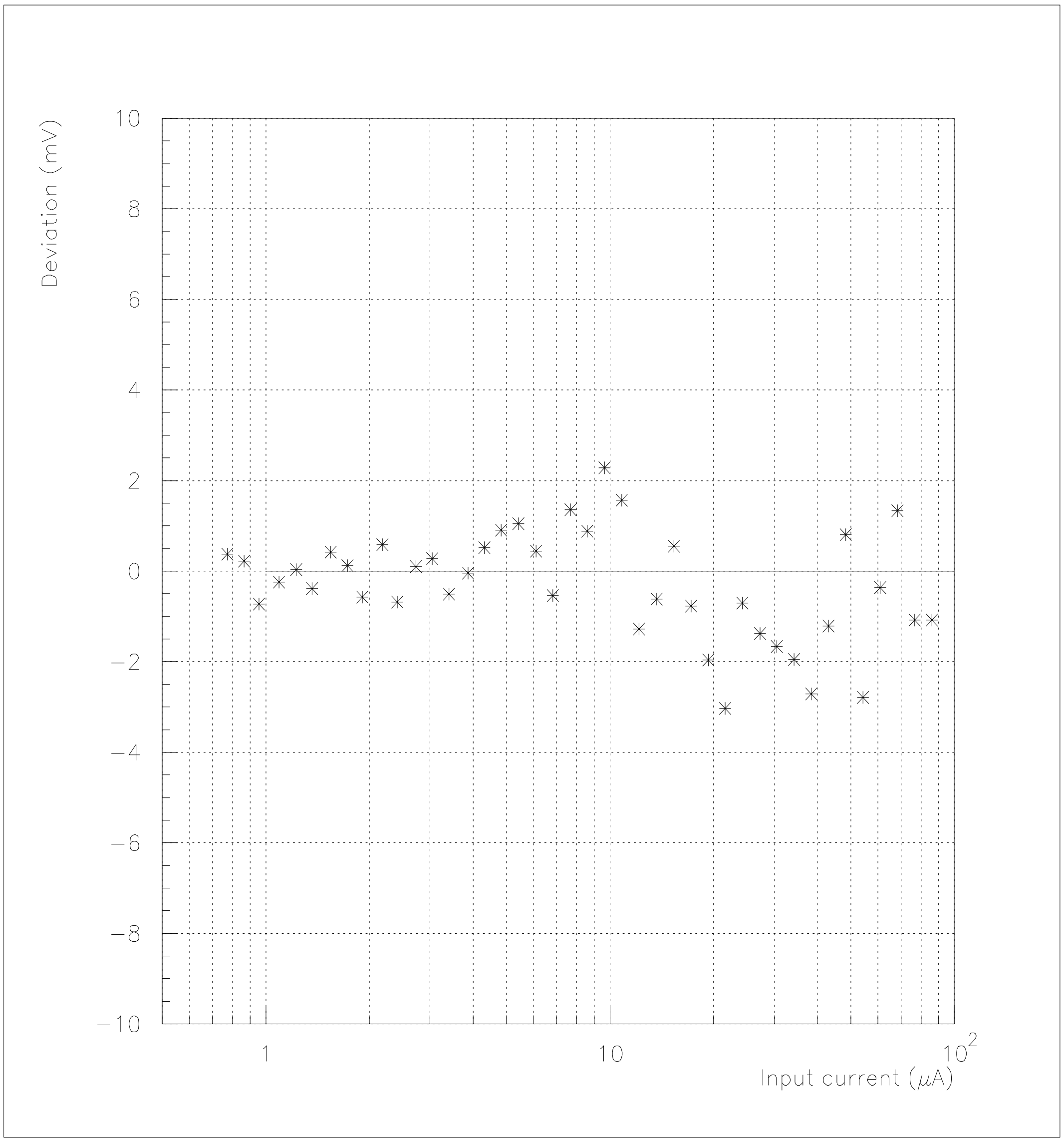

Figure 5: The amplifier non linearity. Deviation from the expected value of the output voltage vs input current

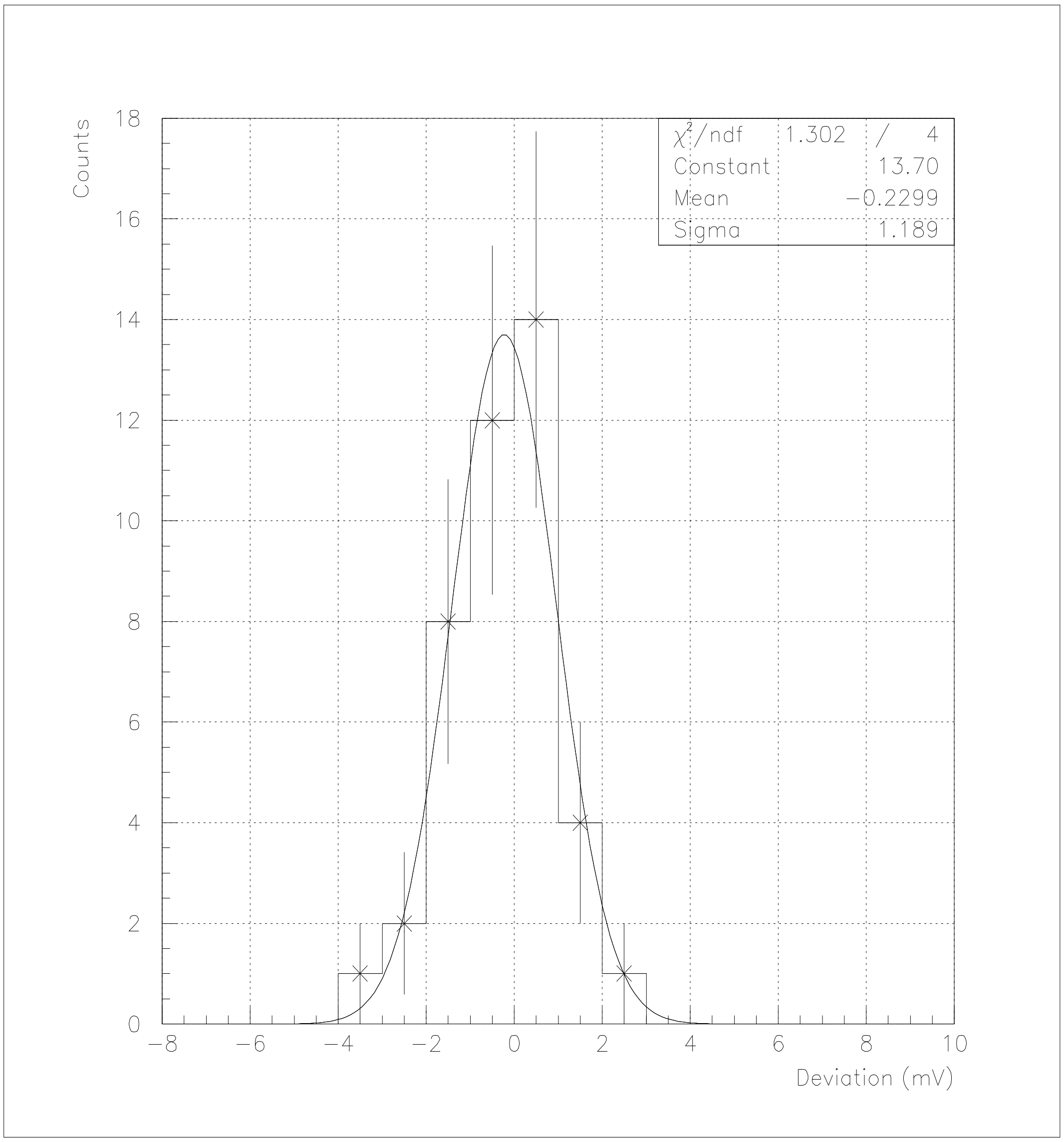

Figure 6: The normal distribution of deviations from linearity (measured output minus expected output): systematic errors are negligible.

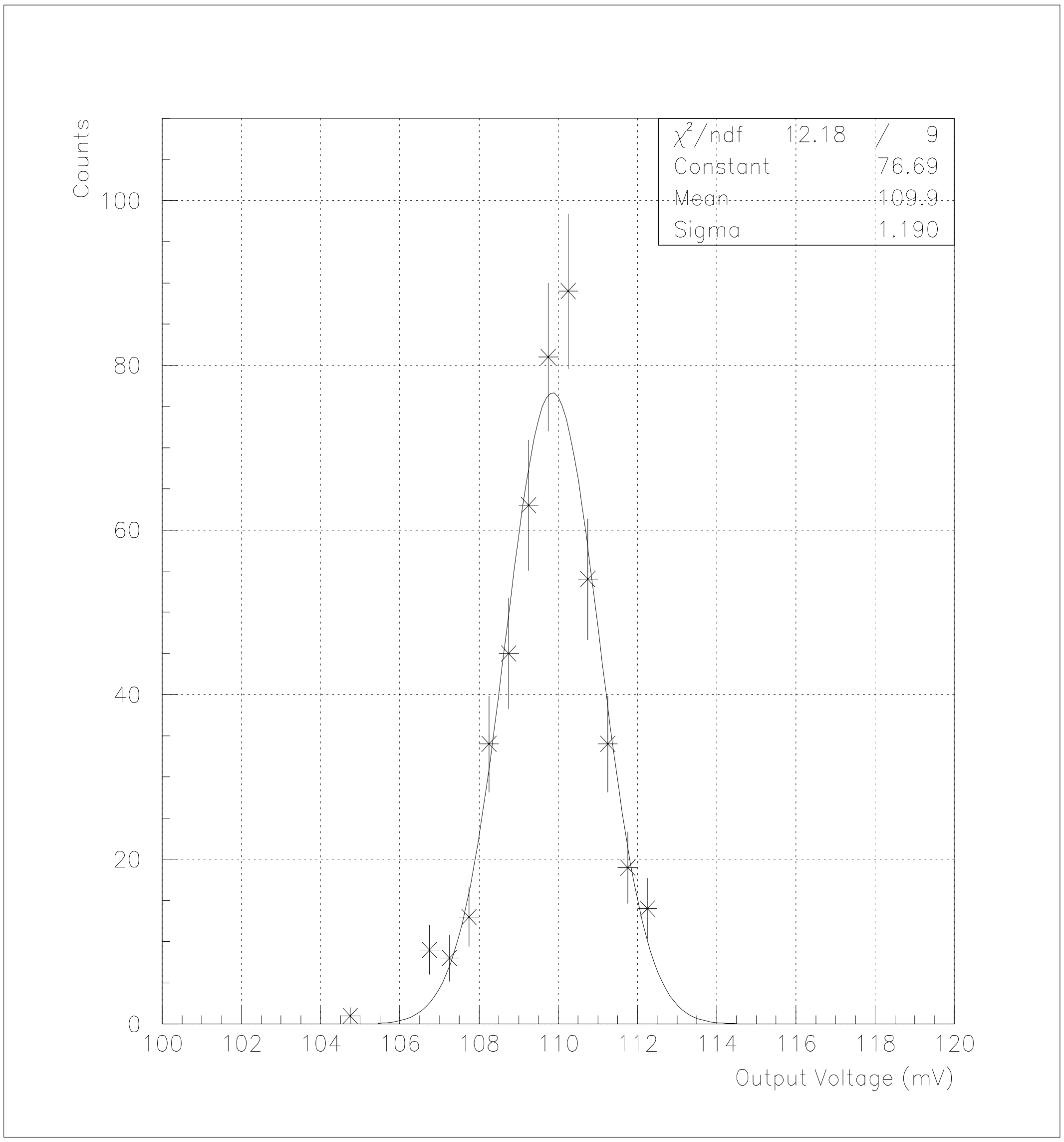

Figure 7: The gain tests for 600 amplifiers. Output voltage distribution for a 3 μA input current pulse.

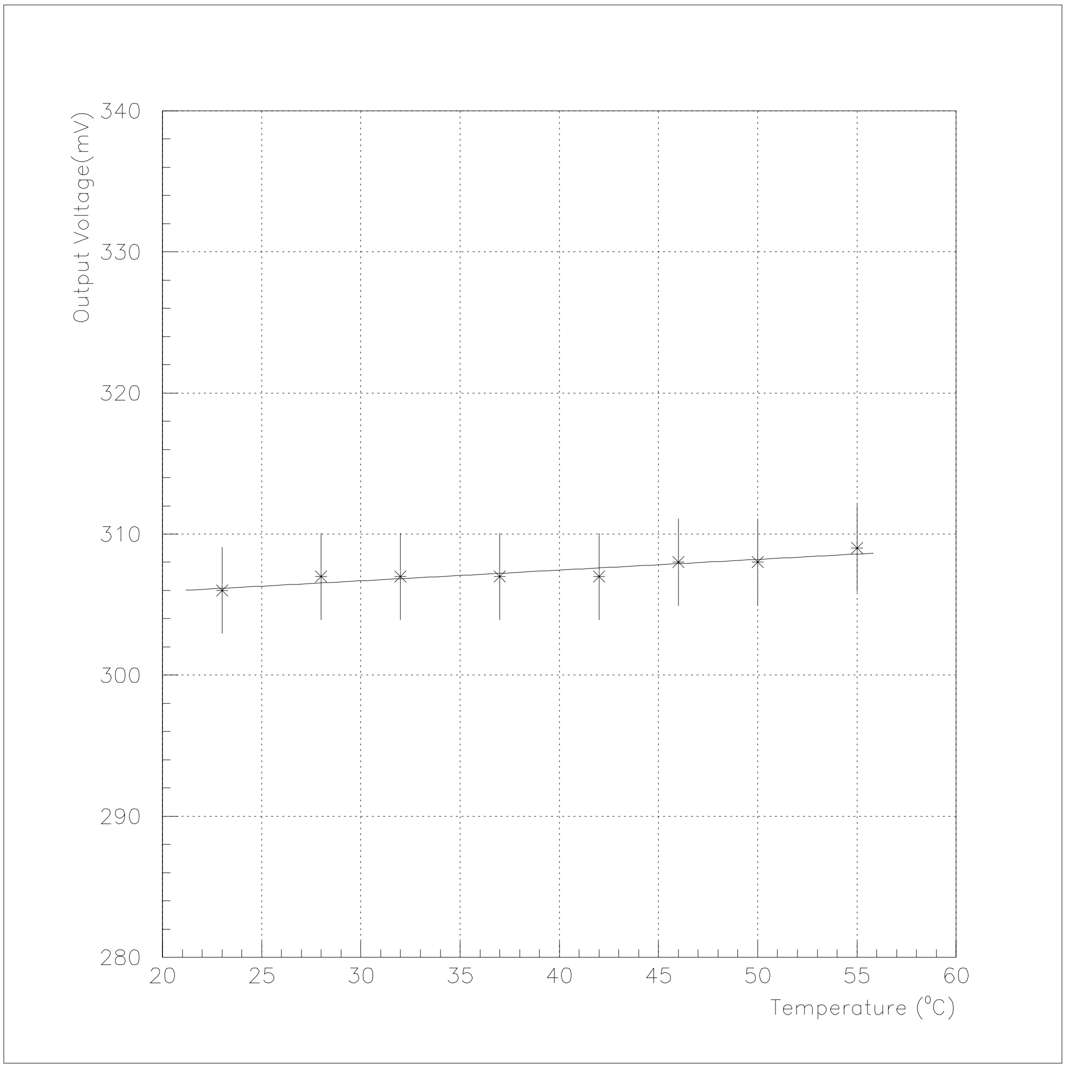

Figure 8: The gain variation with temperature: output voltage vs temperature.

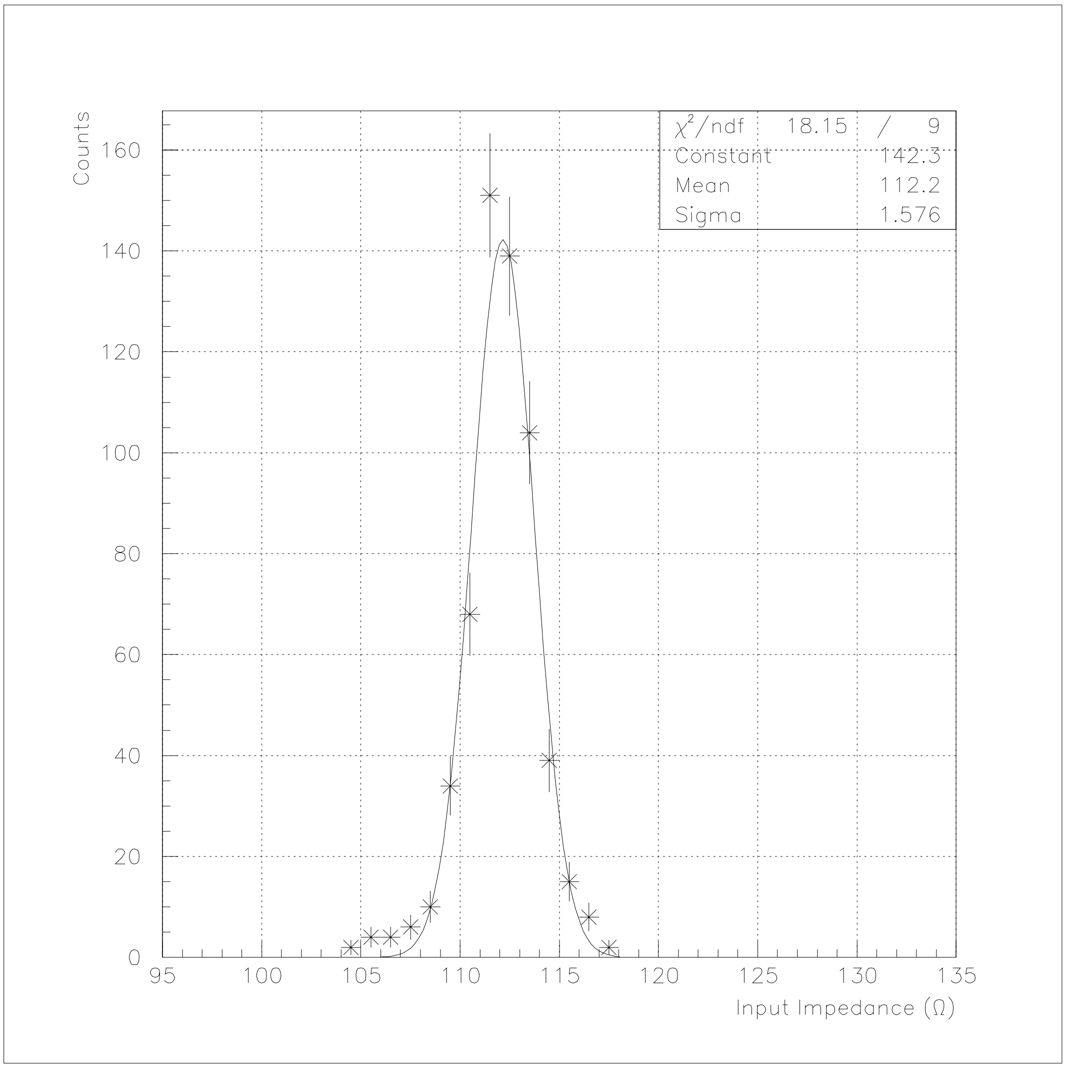

Figure 9: The input impedances distribution of 600 amplifiers.

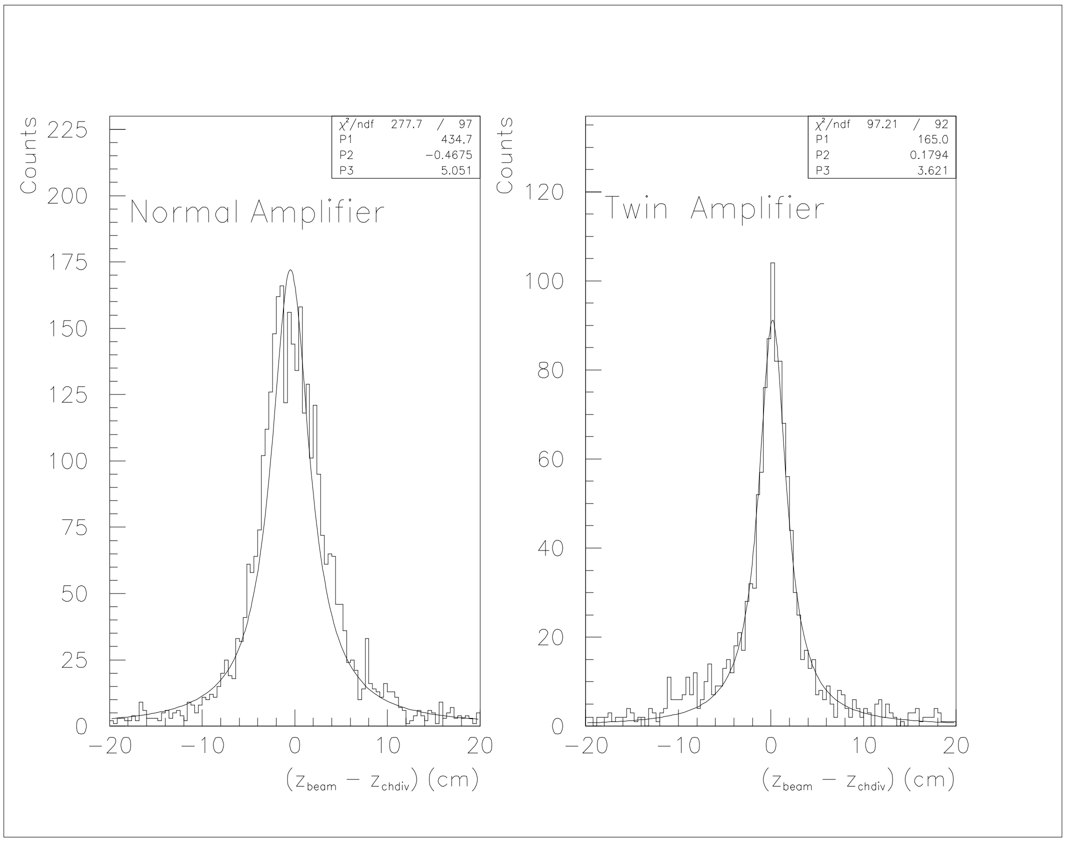

Figure 10: The distribution of the differences between the z coordinate measurement from the beam monitor and from the charge division method with a normal (a) and a twin (b) amplifier. The fit with a lorentzian distribution is superimposed.

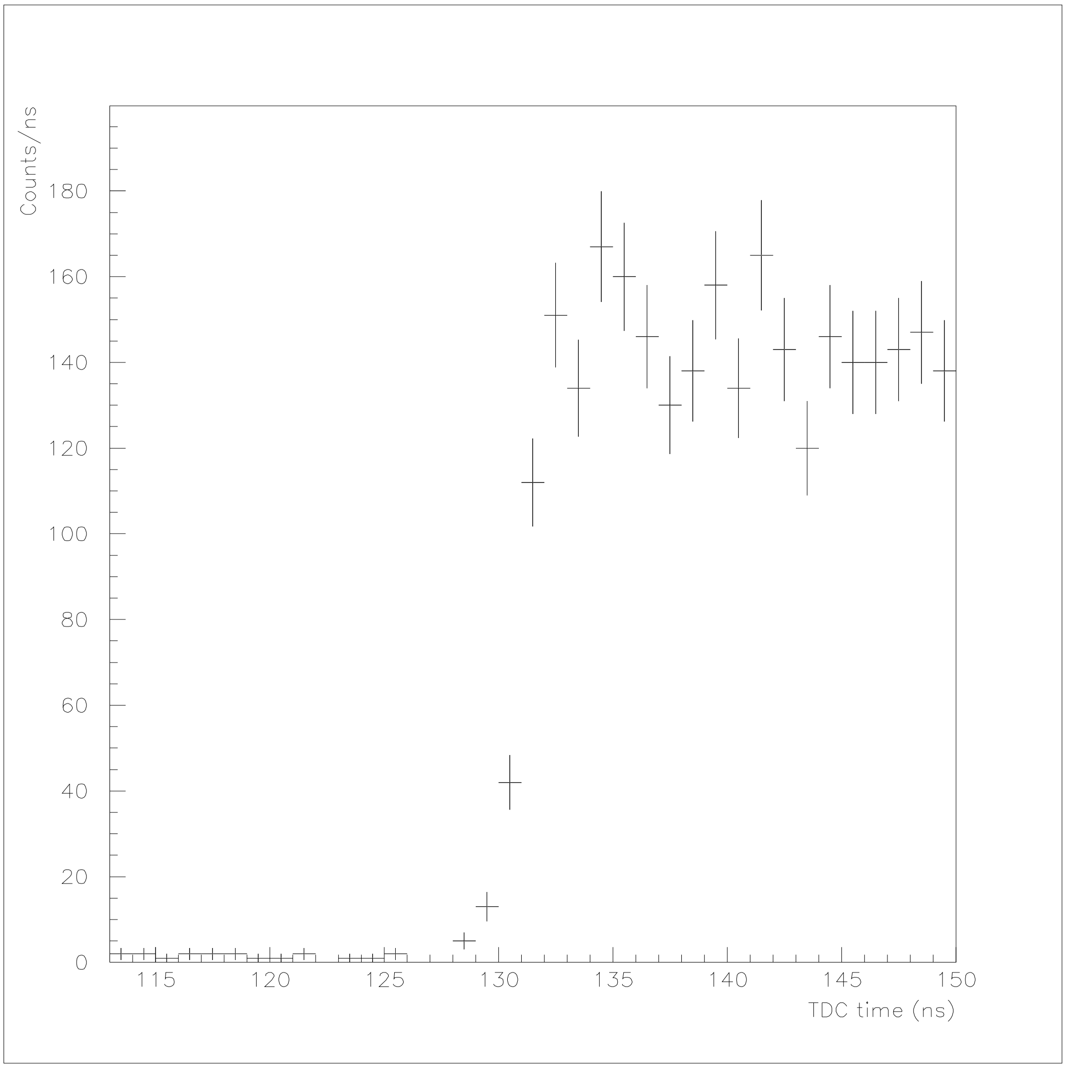

Figure 11: The rise drift time

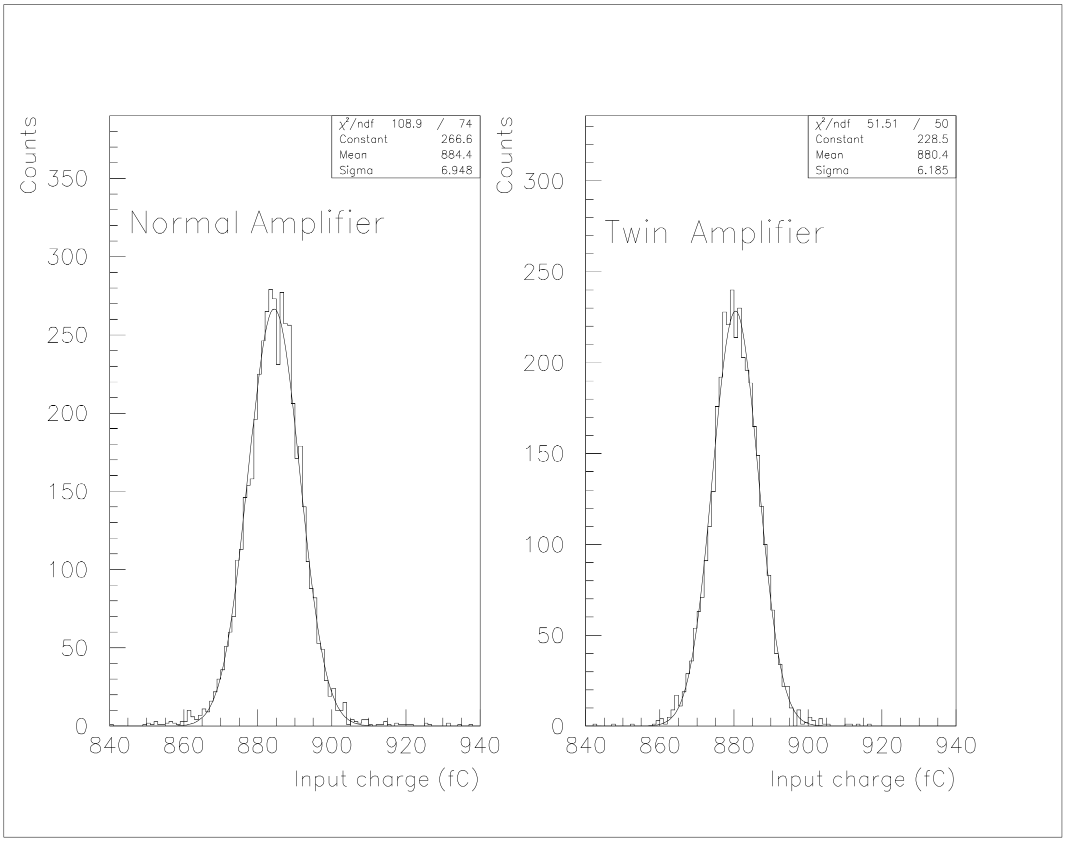

Figure 12: The distribution of the reconstructed input pulses for the normal (a) and the twin (b) amplifier.